Targeted and Interactome Proteomics Revealed the Role of PHD2 in Regulating BRD4 Proline Hydroxylation

Authors

Luke Erber, Ang Luo, and Yue Chen

Correspondence

YueChen@umn.edu

Graphical Abstract

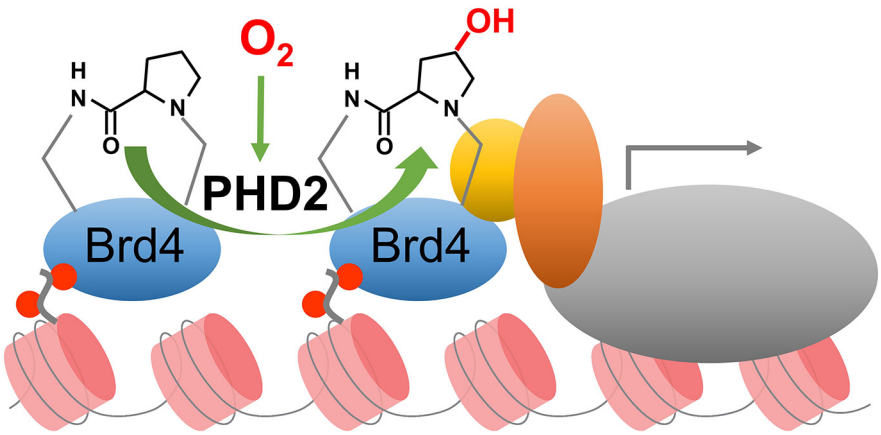

In Brief

Targeted quantification assays using MS-based parallel-reaction monitoring and biochemical analysis revealed PHD2 as a key regulatory enzyme of BRD4 proline hydroxylation. Quantitative MS-based interactome and biochemical analyses revealed the functional significance of the proline hydroxylation modification pathway in BRD4-mediated protein-protein interactions and transcriptional activation. Taken together, these results provided mechanistic insights into the oxygen-dependent modification of BRD4 and revealed new roles of the proline hydroxylation pathway in regulating BRD4-mediated protein-protein interaction and gene expression.

Highlights

- BRD4 interaction with prolyl hydroxylase domain proteins.
- Stoichiometric dynamics and site-specific regulation of BRD4 proline hydroxylation.
- BRD4 interactome analysis in response to prolyl hydroxylase activity.
- Proline hydroxylation pathway regulation of BRD4-mediated transcriptional activity.

Erber et al., 2019, Molecular & Cellular Proteomics *18*, 1772–1781

https://doi.org/10.1074/mcp.RA119.001535

Targeted and Interactome Proteomics Revealed the Role of PHD2 in Regulating BRD4 Proline Hydroxylation*[S]

Luke Erber, Ang Luo, and Yue Chen‡

Proline hydroxylation is a critical cellular mechanism regulating energy homeostasis and development. Our previous study identified and validated Bromodomain-containing protein 4 (BRD4) as a proline hydroxylation substrate in cancer cells. Yet, the regulatory mechanism and the functional significance of the modification remain unknown. In this study, we developed targeted quantification assays using parallel-reaction monitoring and biochemical analysis to identify the major regulatory enzyme of BRD4 proline hydroxylation. We further performed quantitative interactome analysis to determine the functional significance of the modification pathway in BRD4-mediated protein-protein interactions and gene transcription. Our findings revealed that PHD2 is the key regulatory enzyme of BRD4 proline hydroxylation and the modification significantly affects BRD4 interactions with key transcription factors as well as BRD4-mediated transcriptional activation. Taken together, this study provided mechanistic insights into the oxygen-dependent modification of BRD4 and revealed new roles of the pathway in regulating BRD4-dependent gene expression. ***Molecular & Cellular Proteomics 18: 1772–1781, 2019. DOI: 10.1074/mcp.RA119.001535.***

Oxygen availability governs the energy homeostasis and development of living organisms. Cellular adaptation to the changes of the oxygen concentration is regulated by diverse signaling and transcriptional mechanisms (1–5). Proline trans-4-hydroxylation (Hyp)[1] is an evolutionarily conserved post-translational modification (PTM) directly involved in oxygen sensing (6–9). The decrease in oxygen concentration decreases the abundance of proline hydroxylation on the substrate proteins, which further alters the protein-protein interactions, downstream signaling and gene expression (10). Such regulatory mechanisms are known to play central roles in diverse cellular pathways including erythropoiesis, angiogenesis, and the activation of cellular survival responses (11–14).

Prolyl hydroxylase domain proteins (PHDs) are one of the major enzyme families that regulate proline hydroxylation in cells (15–17). The enzymatic activity of the PHDs require cofactors including oxygen, iron (Fe^{2+}), and alpha-ketoglutarate, which makes PHDs an ideal sensor for cellular metabolic states. There are three major PHD family proteins PHD-1, 2, 3 (also known as EGLN-2, 1, 3 respectively) in mammals. PHD2 is usually more abundant than PHD1 and PHD3 in cells and tissues, whereas PHD1 predominates in testis and PHD3 is highly expressed in the heart (18). The α-subunits of the hypoxia-inducible factor (HIF) complex are important targets of PHD proteins. PHD-mediated hydroxylation of HIF-α proteins promotes its interaction with ubiquitin E3 ligase von-Hippel-Lindau (pVHL), which leads to HIF-α poly-ubiquitination and rapid degradation by proteasome under normoxia conditions (19–22). Low oxygen concentration under hypoxia conditions inhibits PHD enzyme activity and further inhibits hydroxylation-dependent degradation of HIF-α proteins. Stabilized HIF-α subunits form a complex with HIF-β proteins and activate the transcription of nearly one hundred genes as central cellular responses to hypoxia (23–25).

Recent functional and system-wide studies have identified several Hyp targets regulated by PHD enzymes including PKM2, AKT, NDRG3, ACC2, FOXO3a, and p53, that regulate diverse cellular pathways involving signaling and energy homeostasis (26–31). Through proteomics-based screening, we previously identified Bromo-domain containing protein 4 (Brd4) as a new Hyp target with a high modification stoichiometry (~60%) at an evolutionarily conserved site P536 (supplemental Fig. S1) (32). In the present study, we applied label-free targeted proteomics analysis with parallel reaction monitoring (PRM) to identify the regulatory enzyme of Brd4 proline hydroxylation and then performed quantitative interactome analysis to reveal the functional significance of the modification on Brd4-mediated transcriptional pathways.

EXPERIMENTAL PROCEDURES

Cell Culture and Transient Transfection—HeLa and 293T cells were cultured in Dulbecco's Modified Eagle Medium (DMEM, ThermoFisher Scientific, Waltham, Massachusetts). Media was supplemented with 10% FBS (Sigma, St. Louis, Missouri), 100IU penicillin, 100 μg/ml streptomycin (Bethyl, Montgomery, Texas). Cells were

From the Department of Biochemistry, Molecular Biology and Biophysics, University of Minnesota, Minneapolis, Minnesota 55455
Received April 30, 2019, and in revised form, June 19, 2019
Published, MCP Papers in Press, June 25, 2019, DOI 10.1074/mcp.RA119.001535

grown at 37 °C in a 5% CO_2 incubator. Transfection in HeLa and HEK293T cells was performed using 1 mg/ml polyethyleneimine (PEI). Transfection was conducted with a 1:3 ratio (μg DNA: μg PEI) in 500 μl OptiMEM (ThermoFisher Scientific).

Plasmids, siRNAs, and Peptides—pFlag-CMV2-Brd4 (1–1362) was a gift from Eric Verdin (Addgene plasmid # 22304, Watertown, Massachusetts). The plasmid containing flag-BRD4 P536A has been previously described (32). c-myc promoter luciferase vector was a gift of Bert Vogelstein (Addgene plasmid #16601). pcDNA-RLuc8 was a gift from Sanjiv Sam Gambhir (Addgene plasmid # 87121). The pc-DNA plasmid vectors containing HA-tagged PHD1, HA-tagged PHD2, and myc-tagged PHD3 were gifts of Do-Hyung Kim. The pLKO.1-puro vector encoding shRNA targeting PHD2, HIf1a, BRD4, and control were purchased from IDT, Coralville, Texas (TRCN0000001045, TRCN0000003810, TRCN0000021424 and respectively). The previously described PHD2 siRNA sequence was purchased from Dharmacon (5′-GACGAAAGCCAUGGUUGCUUG-3′) (33). Control siRNA was MISSION® siRNA Universal Negative Control (Sigma, SIC001). siRNA transfection was performed using with DharmaFECT 1 Transfection Reagent according to the manufacturer's instructions (Dharmacon, Lafayette, Colorado).

Generation of Stable Knockdown Cell Lines—To establish stable cell lines, shRNA plasmids were cotransfected into 293T cells or HeLa cells together with psPAX2 and pMD2.G at the ratio of 4:3:1. Forty-eight hours after transfection, the cell medium containing the lentivirus was filtered and used to infect the target cells with the help of polybrene (8 μg/ml). Twenty-four hours after infection, the cells were transferred into medium containing 2 μg/ml puromycin for selection. When most of the cells became resistant to puromycin, the concentration of the drug was reduced to 1 μg/ml and the cells were used for further experiments. Knockdown was validated by Western blotting and PCR.

Immuno-purification and Western Blot Analysis—293 T cells were grown to 60% confluence and transfected with expression plasmids. Sixteen hours after transfection, cells were treated with or without dimethyloxalylglycine (DMOG) (Cayman Chemical, Ann Arbor, Michigan) for 6 h. Twenty-four hours post-transfection, cells were washed with PBS and lysed with 10 mM Tris-HCl pH 8.0, 1 mM EDTA, 1% Triton X-100, 150 mM NaCl and protease inhibitor (Sigma). Cell lysate's protein concentration was measured using Bradford assay (ThermoFisher Scientific). To conduct immunoprecipitation, cell lysates were incubated with antibody-coupled beads, either anti-FLAG M2 affinity gel (Sigma) or anti-HA magnetic beads (ThermoFisher Scientific), for 16 h at 4 °C. Subsequently, the beads were washed 3 times with 0.1% Tween-20 in 1× PBS. Elution was performed with sample loading buffer (62.5 mM Tris-HCl pH 6.8, 2% sodium dodecyl sulfate, 0.05% bromphenol blue, 10% glycerol, and 5% beta-mercaptoethanol) and boiling for 5 min. For Western blotting, equal amounts of input and immunoprecipitation protein were separated by SDS-PAGE, transferred to PVDF membranes (Millipore, Burlington, Massachusetts) and detected using anti-flag, anti-tubulin, anti-Hif1α (Sigma), anti-HA (Biolegend, San Diego, California), anti-myc (ThermoFisher Scientific), anti-actin (VWR, Radnor, Massachusetts), anti-CDK9 (Cell Signaling, Danvers, Massachusetts), anti-PHD2 (Novus Biologicals, Centenial, Colorado), anti-mcm5 and anti-CDK1 (Bethyl) antibodies according to the manufacturer instructions.

BRD4 MS-based Interactome Analysis—Hela cells stably expressing siControl or siPHD2 were transiently transfected with wild-type BRD4 or BRD4 P536A. To ensure reproducibility, three biological replicate samples were prepared for each condition and empty vector controls were included to filter out false positive bait interactors. After transfection, cell lysis and immunoprecipitation were carried out and the immunoprecipitation elutions were loaded into SDS-PAGE gel for protein separation followed by in-gel trypsin (Promega, Madison, Wisconsin) digestion as previously described (34).

Peptides of each biological replicate were injected into the nano-LC Proxeon (Easy-nLC 1000, Thermo Scientific) coupled to an Orbitrap Fusion mass spectrometer (Thermo Scientific). The peptides were loaded onto an in-house packed C18 column (15 cm × 75 μm, ReproSil-Pur Basic C18, 2.5 μm, Dr. Maisch GmbH, Ammerbuch, Germany) and separated with a 60-min gradient using HPLC buffer A (0.1% formic acid) and buffer B (acetonitrile, 0.1% formic acid). The LC-MS analysis was performed in a data-dependent mode. The survey scan was acquired with a resolution setting of 60,000 at 200 *m/z*. Dynamic exclusion was enabled with an exclusion duration for 15 s. The 12 most intense precursor ions were selected for HCD fragmentation using activation energy of 35% in the ion trap.

The raw mass spectrometry data was searched with MaxQuant (version 1.5.3.12) using default parameters (35), against the human Uniprot database (downloaded on 2014/04/14, with 69,081 sequences) with trypsin selected as the protease that cleaves peptide bonds at the C terminus of lysine and arginine and allows for a maximum of two missing cleavages. Variable modifications of methionine oxidation, protein N-terminal acetylation and the fixed modification of cysteine carbamidomethylation were selected. The precursor ion and fragment ion mass tolerance of 4.5 ppm and 0.5 Da were selected, respectively. The False Discovery Rate (FDR) was set to 1% at the protein, peptide and site levels with a minimum peptide length of 6 and a minimum Andromeda score of 40. For protein identification, a minimum of two peptides was required. Default label-free quantification (LFQ) parameters were selected for label-free quantification with normalized protein intensities as the output.

The protein LFQ intensities were processed using the Perseus software suite (36). The data was Log2 transformed and filtered (37). A two-tailed, two-sample *t* test was performed to compare protein abundance among groups (38). Statistically, significant enrichment was determined with a Benjamini-Hochberg corrected FDR cutoff of 0.05. To further reduce false positive identifications, we filtered these interactions, removing any identifications that also presented in the control immunoprecipitation samples.

Targeted Quantification of BRD4 Proline Hydroxylation—To measure the change in proline hydroxylation abundance, the Flag-BRD4 vector was expressed in 293T cells and cotransfected with either HA-PHD1, HA-PHD2 or myc-PHD3 vectors or treated with 1% oxygen using a hypoxia chamber (Biospherix Ltd, Parish, NY). To measure the change in proline hydroxylation on PHD2 knockdown, 293T cells stably expressing control shRNA and PHD2 shRNA were generated as previously described (31). Cells were lysed and BRD4 was immunoprecipitated using either anti-flag agarose beads or with 1 μg BRD4 antibody (Millipore) and protein A/G beads as previously described (32). Protein was separated with SDS-PAGE, stained with Coomassie blue (National Diagnostics, Atlanta, Georgia) and digested with trypsin as previously described (34).

Tryptic peptides were analyzed by LC-MS/MS as previously described (32). Peptides were injected into the nano-LC Proxeon (Easy-nLC 1000, Thermo Scientific) coupled to an Orbitrap Fusion mass spectrometer (Thermo Scientific). The peptides were loaded onto an in-house packed C18 column (15 cm × 75 μm, ReproSil-Pur Basic C18, 2.5 μm, Dr. Maisch GmbH) and separated with a 60-min gradient using HPLC buffer A (0.1% formic acid) and buffer B (acetonitrile,

[1] The abbreviations used are: Hyp, proline trans-4-hydroxylation; BRD4, bromodomain-containing protein 4; PTM, post-translational modification; PHDs, prolyl hydroxylase domain proteins; HIF, hypoxia inducible factor; pVHL, von-Hippel-Landau; PRM, parallel reaction monitoring; DMOG, dimethyloxalylglycine; LFQ, label-free quantification; AML, acute myeloid leukemia.

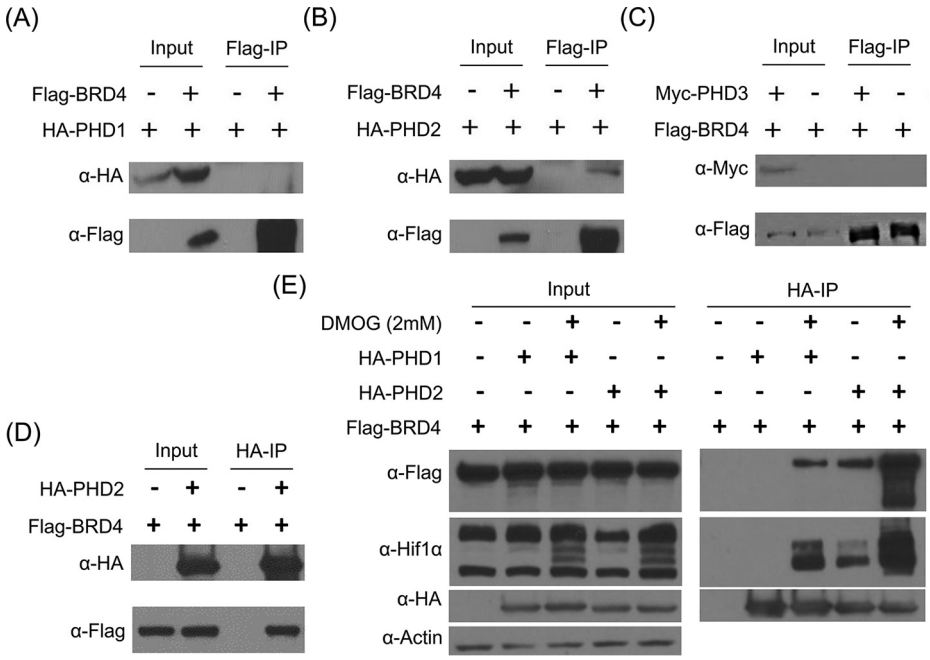

FIG. 1. **Screening for BRD4 interactions with Prolyl Hydroxylase Domain proteins.** *A–C*, Western blot analysis showing flag-IP results following coexpression of Flag-tagged BRD4 with HA-tagged PHD1, PHD2, and myc-tagged PHD3. Only co-IP in 1B is significant, suggesting BRD4 bind preferentially to PHD2. *D*, Western blot analysis showing HA-IP results following coexpression of HA-tagged PHD2 with Flag-tagged BRD4. *E*, Western blot analysis showing HA-tag IP results following coexpression of Flag-tagged BRD4 with HA-tagged PHD1, HA-tagged PHD2, and treatment with 2 mM DMOG. Co-IP following DMOG treatment reveals a significant increase in BRD4 binding to PHD2.

0.1% formic acid). Label-free Parallel Reaction Monitoring (PRM) was used to monitor precursor ions to determine specific HPLC elution peaks (Tier 3) (39). The precursor ions with the mass to charge ratios of 663.0288 and 668.3604 with the transition states of 244.1656 and 260.1605, corresponding to the unmodified and hydroxylated BRD4 peptides respectively, were selected for targeted HCD fragmentation using activation energy of 35%. Precursor and fragment ion spectra were acquired in the Orbitrap (39). HPLC chromatogram peak areas of targeted ions were calculated to determine the prevalence of modified peptides using the default ICIS algorithm in Qual Browser with 9-points Gaussian smoothing. The stoichiometry was calculated with the following formula: %Hyp modified = (Peak area of Hyp peptide)/(Peak area of Hyp peptide + Peak area of Unmodified peptide). Three biological replicates were analyzed under each condition and two-tailed unpaired Student's *t* test was applied to determine statistical significance.

Bioinformatic Analysis—The functional annotation enrichment analysis for the proteins enriched with BRD4 was performed with the online tool DAVID Bioinformatics Resources 6.8 (40, 41). The BRD4 interaction map was generated using Cytoscape (version 3.7) (42).

Luciferase Assay—293 T cells in 24-well plates were transiently transfected with c-Myc Firefly luciferase reporter vector together with a Renilla luciferase vector and siRNA for BRD4. After 48 h, two sets of cells were transfected with either wild-type BRD4 or BRD4 P536A vectors, whereas one set of cells was treated with 50 μM JQ1 for 24 h before harvesting. Luciferase activity was measured using the Dual-GloLuciferase Assay on the GloMax Microplate Reader (Promega).

Quantitative Real-time PCR—Total RNA from three biological replicates for each treatment condition was isolated from cells using TRIzol Reagent (Invitrogen, Carlsbad, California) according to the manufacturer's instructions. For each sample, 2 μg raw RNA was reverse-transcribed into cDNA with M-MLV Reverse Transcriptase (Promega) in a 25 μl reaction system. The reverse-transcription product was further diluted to 150 μl. Two μl was used as a template for each qRT-PCR reaction. The reaction was performed on CFX96 Touch™ Real-Time PCR Detection System (BioRad, Hercules, California) and the reagent was Luna® Universal qPCR Master Mix (New England Biolabs, Ipswich, Massachusetts, M3003). qRT-PCR data were collected for each primer pair in triplicate and was analyzed for RNA expression. GAPDH was used as the reference gene for normalization. All reactions were run in triplicate. The primers for qRT-PCR are listed in the Supplementary Information (supplemental Table S5).

Experimental Design and Statistical Rationale—For the Quantitative real-time PCR, luciferase assays, targeted quantification of BRD4 proline hydroxylation, samples from at least three biological replicates were isolated to account for biological variability. Data were collected in triplicate to account for technical variation. For quantification, each experiment was normalized to vehicle control and the normalized values were averaged. Statistical significance was calculated using two-tailed Student's *t* test, as described in each figure legend.

For MS-based interactome analysis, empty vector controls were included as sham controls to filter out false positive bait interactors. To ensure reproducibility, three biological replicate samples were prepared for each experimental condition to account for biological variation. Sample processing for all conditions was performed in parallel and with the same batch of reagents for maximal reproducibility of protein enrichment, peptide digestion and data acquisition by mass spectrometry. All mass spectrometry data were analyzed using the same database FASTA file (Uniprot Human proteome database downloaded on 2014/04/14, with 69,081 sequences) and the same MaxQuant version (1.5.3.12).

RESULTS

Candidate Screening Analysis of BRD4-PHD Interactions—To identify the PHD enzyme that regulates BRD4 prolyl hydroxylation, we first performed a candidate screen to identify the prolyl hydroxylase that preferentially interacts with BRD4. By expressing individual PHD family proteins with BRD4, we performed coimmunoprecipitation (IP) and Western blot analysis. Our data showed that BRD4 preferentially interacted with PHD2 compared with PHD1 or PHD3 (Figs. 1*A*–1*C*). The interaction between BRD4 and PHD2 was further confirmed by a reciprocal coimmunoprecipitation (Fig. 1*D*). To determine if the interaction between BRD4 and PHD2 was dependent on PHD2 enzymatic activity, we applied a sub-

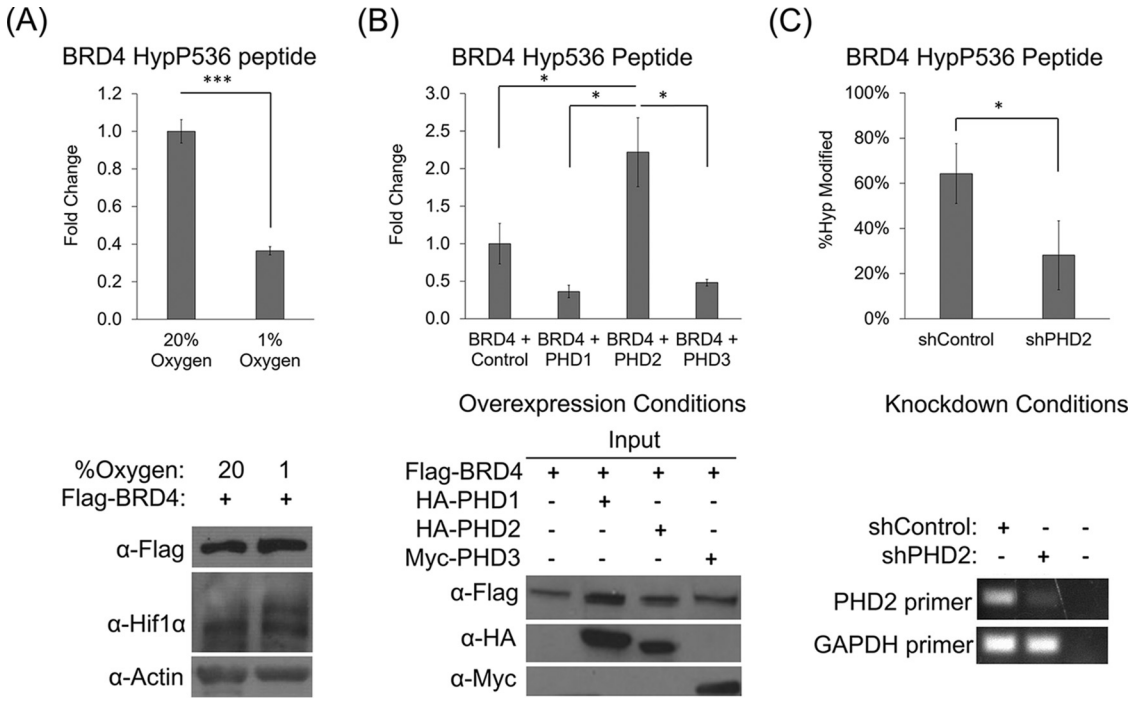

FIG. 2. **Stoichiometric dynamics and site-specific regulation of BRD4 proline hydroxylation.** *A*, Targeted analysis of BRD4 Hyp536 abundance in response to the hypoxia treatment. The Hyp536 peptide precursor ion peak area of each sample was normalized. Protein expression after oxygen treatment was confirmed by Western blotting. BRD4 Hyp536 abundance changes in response to oxygen deficiency. *B*, The dynamics of BRD4 P536 hydroxylation abundance following the overexpression of PHD1, PHD2, and PHD3. Only overexpression of PHD2 leads to a significant increase in BRD4 P536 hydroxylation. *C*, The dynamics of BRD4 P536 hydroxylation abundance following the knockdown of PHD2 indicates PHD2 inhibition leads to decreased BRD4 P536 hydroxylation. * $p < 0.05$, *** $p < 0.001$, Student's *t* test assuming unequal variance.

strate-trapping strategy as previously reported (43). This strategy used dimethyloxalylglycine (DMOG) treatment to stabilize the PHD enzyme-substrate intermediate complex and therefore enabled the identification of new PHD interactions that depend on PHD enzymatic activities. Our data showed that treatment with DMOG indeed resulted in a dramatically increased affinity of PHD2 with BRD4 (Fig. 1*D*, supplemental Fig. S2). These observations indicate that PHD2 is the major prolyl hydroxylase that interacts with BRD4 *in vivo*.

Site-specific Regulation of BRD4 Proline Hydroxylation—To determine the site-specific dynamics of BRD4 Hyp536, we developed a targeted quantification assay with parallel reaction monitoring (PRM) (32). This approach selectively monitors the abundance of the BRD4 Hyp peptide (containing Hyp536) and its corresponding unmodified peptide based on targeted fragmentation in LC-MS analysis and then compares that stoichiometric dynamics of BRD4 proline hydroxylation under different conditions. Using this strategy, we first aimed to determine whether changes in the cellular microenvironment regulated the site-specific dynamics of BRD4 proline hydroxylation. To this end, 293T cells were cultured under 1 and 20% oxygen conditions and Flag-tagged BRD4 were purified, followed by tryptic digestion and PRM-based targeted LC-MS analysis. Our data showed that hypoxia treatment (1% O_2) significantly reduced BRD4 P536 Hyp stoichiometry by about 60% (Fig. 2*A*), confirming that oxygen is required for BRD4 proline hydroxylation. To determine the PHD protein that regulates BRD4 proline hydroxylation, we performed overexpression of individual PHD proteins and then measured the changes in BRD4 Hyp stoichiometry with PRM-based targeted LC-MS analysis. Our data showed that only overexpression of PHD2 resulted in a significant increase of BRD4 proline hydroxylation by 2-fold. Interestingly, overexpression of PHD1 and PHD3 led to a nearly 2-fold decrease in the abundance of BRD4 proline hydroxylation (Fig. 2*B*). These data suggest that PHD2 is the main prolyl hydroxylase that regulates BRD4 proline hydroxylation. Next, we tested whether BRD4 hydroxylation on P536 is dependent on PHD2 protein. To this end, we knocked down PHD2 using shRNA, enriched for endogenous BRD4 through immunoprecipitation and monitored P536 proline hydroxylation through PRM-based targeted LC-MS analysis. Indeed, we observed a significant decrease in BRD4 Hyp stoichiometry on PHD2 knockdown (Fig. 2*C*). In conclusion, these data suggest that PHD2 is the major regulatory enzyme of BRD4 P536 hydroxylation *in vivo*.

Hydroxylation of P536 Does Not Affect BRD4 Stability—To determine the functional significance of BRD4 P536 hydroxylation, we first investigated whether proline hydroxylation affects BRD4 protein abundance. To this end, HEK293 cells

were treated by prolyl hydroxylase inhibitor DMOG or hypoxia (1% O_2 for 6 and 16 h). The Western blot analysis showed that neither hypoxia nor PHD inhibition treatment led to a change in BRD4 protein abundance (supplemental Fig. S3*A*, S3*B*). This data suggested that changes in BRD4 proline hydroxylation by chemical treatment or hypoxia does not affect its protein stability.

Prolyl Hydroxylation Regulates BRD4 Function Through Distinct Protein-Protein Interactions—Given the well-established role of proline hydroxylation in regulating protein folding and protein-protein interactions, we hypothesized that BRD4 proline hydroxylation may affect its interactions with other binding partners and result in changes in downstream activities. To test the hypothesis, we performed a quantitative analysis of the BRD4 interactome and measured proline hydroxylation dependent BRD4 interactions. We performed two orthogonal experiments and used both site-specific mutation and enzyme-mediated inhibition to identify proline hydroxylation dependent interactors. To mimic site-specific inhibition of BRD4 proline hydroxylation, we followed previous studies and prepared a plasmid expressing a BRD4 P536A mutant using site-directed mutagenesis (26–31). To study enzyme-mediated, inhibited BRD4 interactions we generated two stable HeLa cell lines. Transfection and selection were performed to prepare both PHD2 knockdown and mock knockdown HeLa cells. Both sets of HeLa cell lines were transfected with either Flag-tagged wild type BRD4, Flag-tagged BRD4 P536A and Flag-tagged empty vector. Following immunoprecipitation, we conducted a label-free analysis of the BRD4 interactome by mass spectrometry. To ensure confident and reproducible quantifications, we confirmed that BRD4 was similarly expressed and enriched in all biological replicates (supplemental Fig. S4*A*, S4*B*).

We used intensity-based label-free quantification to compare the relative abundance of BRD4 interactors and determined significant BRD4 interactors with the Student's *t* test. From this approach, our analysis identified 437 BRD4-specific interacting proteins over the Flag-tagged empty-vector control immunoprecipitation (supplemental Table S1). We removed all proteins commonly identified under both BRD4 and control immunoprecipitations as stringent filtering criteria to reduce false positive nonspecific BRD4 interactors. After filtering, we identified 61 proteins uniquely enriched with wild-type BRD4. Previously well-known BRD4 interactors such as CDK9, CCNT1, RSF1, Histone H4, and WHSC1 were found to be significantly enriched in our dataset with a high degree of reproducibility, indicating an efficient coverage of BRD4-specific interactomes (supplemental Fig. S5*A*, supplemental Table S2).

To characterize BRD4 interactome, we performed annotation enrichment analysis with Gene Ontology. Our results showed that BRD4 interactors were highly enriched in biological processes including translational initiation (adj $-\log_{10}p$ = 65.01), mRNA splicing (adj $-\log_{10}p$ = 40.65), gene expression (adj $-\log_{10}p$ = 15.90), viral process (adj $-\log_{10}p$ = 7.06), nucleosome assembly (adj $-\log_{10}p$ = 5.63), DNA repair (adj $-\log_{10}p$ = 3.64) and cell division (adj $-\log_{10}p$ = 3.19) (Fig. 3*A*). Enrichment of these biological processes among the BRD4 interactors agreed well with the current knowledge of BRD4 function in regulating gene transcription and RNA processing (44).

We further performed quantitative interactome analysis to compare the dynamic changes in interactions between BRD4 WT and P536A mutant. Our data showed that over 70% of BRD4 interacting proteins interacted with both BRD4 WT and BRD4 P536A, indicating that the majority of the interactome was not affected by BRD4 site-specific substitution. Interestingly, when we quantitatively compared the wild-type BRD4 and BRD4 P536A interactomes, we found 9 proteins were significantly enriched with wild-type BRD4 and a similar number of proteins were enriched with BRD4 P536A mutant (Fig. 3*B*). To assess whether the interactome differences between BRD4 WT and BRD4 P536A were because of change in protein binding partners rather than inherent batch-to-batch variability, we assessed inter- and intra-sample correlation. The protein LFQ intensities for BRD4 WT and BRD4 P536A replicate samples had greater R-squared correlation values than when comparing sample correlation between BRD4 WT and BRD4 P536A (supplemental Fig. S6*A*–S6*D*). This data suggests that site-specific mutation of BRD4 P536 significantly altered its interactions with specific groups of binding proteins and likely resulted in changes in downstream activities. Gene ontology classification showed that interacting protein that had a significant loss in interactions with BRD4 on site-specific substitution of P536 were highly enriched with transcription-related factors (Fig. 3*C*).

To conclusively determine the critical function of site-specific hydroxylation on BRD4 P536, we performed quantitative interactome analysis with enzyme-mediated inhibition of BRD4 proline hydroxylation. We demonstrated above that PHD2 is the major regulatory enzyme that is required for BRD4 proline hydroxylation. We reasoned that if the changes observed between BRD4 WT and BRD4 P536A were because of site-specific proline hydroxylation and not simply the presence of proline itself, PHD2 knockdown should obliterate the differences in interactomes between BRD4 WT and BRD4 P536A mutant. On the other hand, under PHD2 knockdown, the BRD4 WT interactome should change, whereas BRD4 P536A interactome should be unaffected. To test this hypothesis, we first performed quantitative analysis to compare the BRD4 WT interactomes between control Hela cells and Hela cells with PHD2 knockdown, we found that PHD2 knockdown significantly affected BRD4 interactions with a small group of proteins (Fig. 3*D*, supplemental Fig. S5*B*, supplemental Table S2–S4). Many of these proteins showed a significant change in interaction with BRD4 in the interactome analysis of BRD4 P536A mutant *versus* WT (Fig. 3*D*). Importantly, among thir-

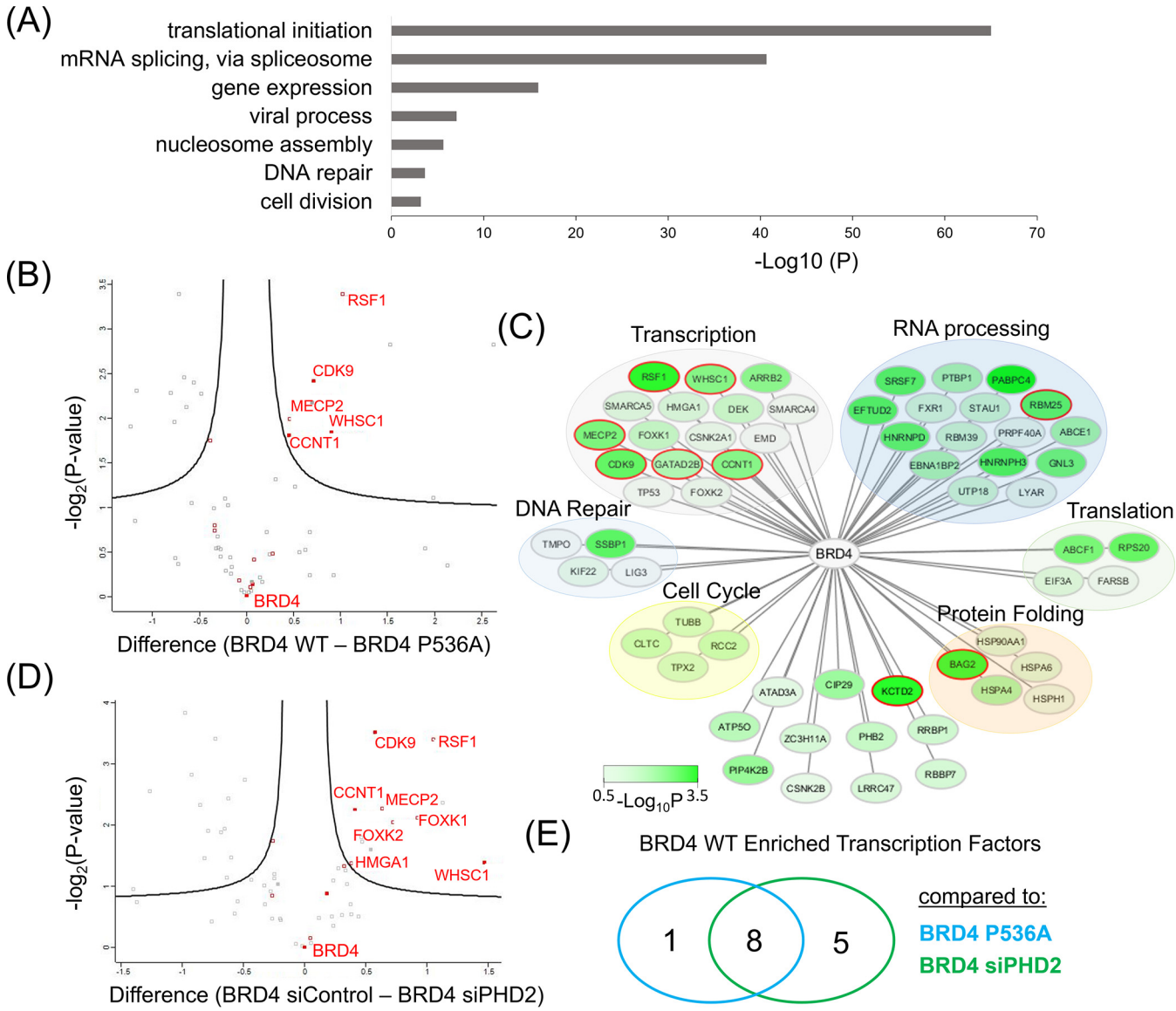

FIG. 3. **BRD4 interactome analysis and its dynamics in response to the regulation of proline hydroxylation pathway.** *A*, Gene Ontology Analysis of the BRD4 interactome with statistical enrichment for biological function (Benjamini-Hochberg adjusted *p* value). *B*, Volcano plot for quantitative analysis of BRD4 WT and P536A mutant interactome at a false discovery rate (FDR) of 0.05 and a minimal coefficient of variation (S0) of 0.1. Proteins on the right side of the volcano plot were significantly enriched with wild-type BRD4 and proteins on the left side were significantly depleted. Proteins having transcription functions were highlighted in red. *C*, BRD4 interaction network that showed differential interactions between WT and mutant BRD4. Transcription factors that were significantly enriched with wild-type BRD4 were highlighted in red. *D*, Volcano plot for quantitative analysis of BRD4 interactome in response to the PHD2 knockdown. *E*, A Venn diagram of transcription factors that significantly lost interaction with BRD4 in the interactome analysis of either BRD4 mutant or PHD2 knockdown experiments.

teen transcription factors that significantly lost interactions with BRD4 on PHD2 knockdown, most of them were also found to have significantly reduced interactions with BRD4 P536A mutant (Fig. 3*E*). To further demonstrate the site-specific role of BRD4 proline hydroxylation in BRD4-mediated protein-protein interaction, we performed quantitative analysis to compare the interactomes of BRD4 WT and P536A mutant under PHD2 knockdown. In contrast to the control cells, our data showed that PHD2 knockdown largely eliminated the difference in BRD4 interactions between BRD4 WT and P536A mutant with interacting proteins including the transcription factors (supplemental Fig. S5*C*, supplemental Table S6). In agreement with this finding, we found that unlike the BRD4 WT interactome, the BRD4 P536A interactome was unaffected by PHD2 knockdown (supplemental Fig. S5*D*, supplemental Table S7). These findings with site-specific and enzyme-mediated inhibitions of BRD4 proline hydroxylation synergistically demonstrated the functionally important role of BRD4 proline hydroxylation on BRD4-mediated protein-protein interactions.

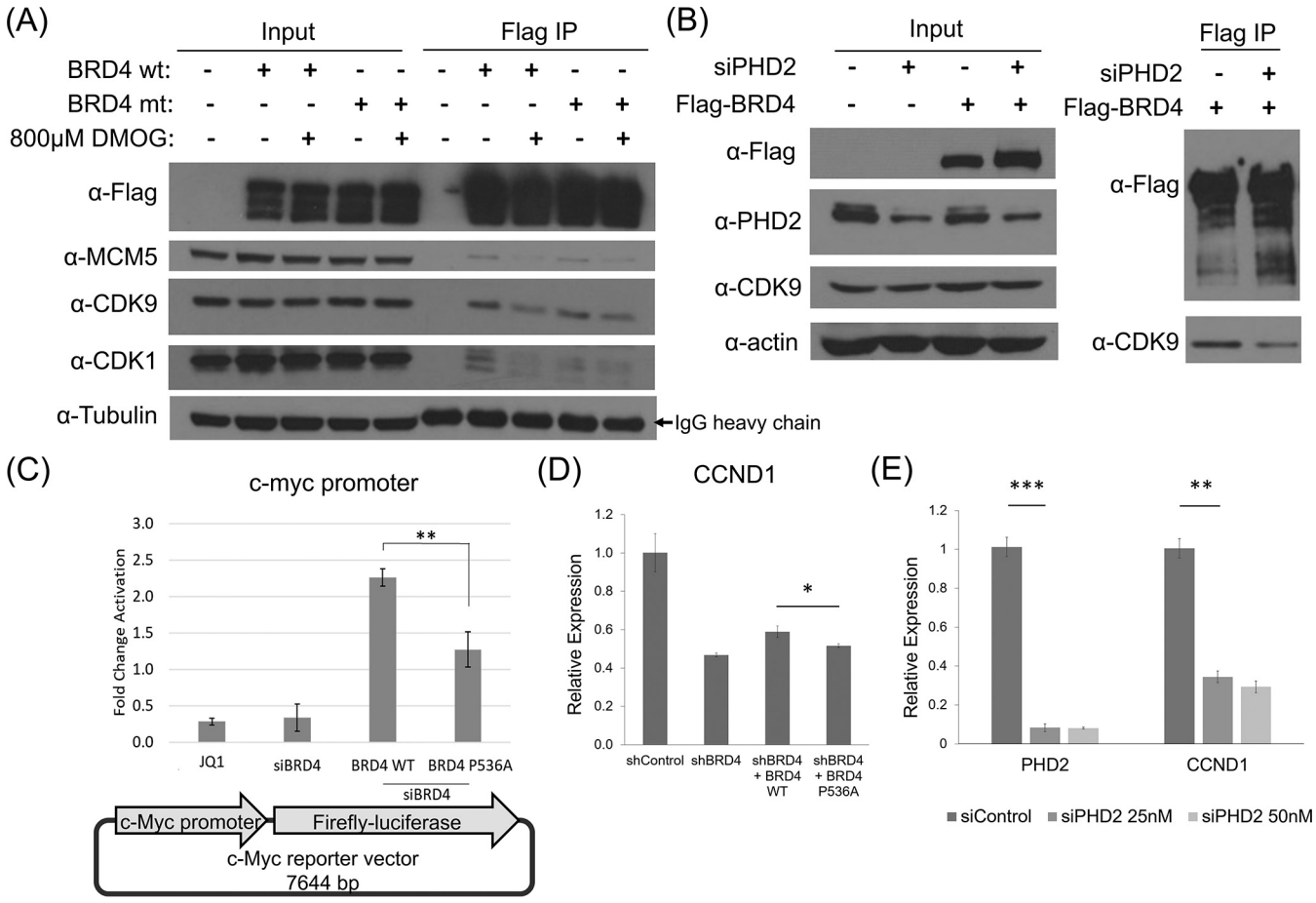

FIG. 4. **Functional validation of the role of proline hydroxylation pathway in regulating BRD4 interactions and BRD4-mediated transcriptional activity.** *A*, Western blotting of BRD4 interactors after DMOG treatment and coimmunoprecipitation with either wild-type BRD4 or BRD4 P536A. Compared with wild-type BRD4, both co-IP with BRD4 mutant and treatment with DMOG exhibit significantly reduced interaction with CDK9, CDK1, and MCM5. *B*, Western blotting of BRD4 interactors with control and PHD2 knockdown. Compared with sham knockdown, co-IP after PHD2 knockdown exhibits significantly reduced interaction between BRD4 and CDK9. *C*, Luciferase assay with a c-Myc responsive reporter constructs presented as fold change compared with the empty vector control treatment. 293T cells were transfected with c-Myc luciferase reporter vector together with a renilla vector, siRNA for BRD4 or cotransfected together with wild-type BRD4 or BRD4 P536A vectors. BRD4 P536A mutant was unable to rescue c-Myc luciferase signal to the same extent as wild-type BRD4. *D*, The quantitative real-time PCR analysis of CCND1 using 293T cells with stable BRD4 knockdown and expression of either wild-type or BRD4 P536A mutant. Data were normalized by GAPDH expression. BRD4 P536A mutant was unable to rescue CCND1 expression to the same extent as wild-type BRD4. *E*, Quantitative real-time PCR analysis showing that knockdown of PHD2 significantly decreased the expression of CCND1. Data were normalized by GAPDH expression. * $p < 0.05$, ** $p < 0.01$, *** $p < 0.001$.

It is well-known that BRD4 interacts and recruits P-TEFb, a complex consisting of CDK9 and CCNT1, to gene promoters and activate RNA polymerase II (RNAPII)-mediated transcriptional activity (45). In our data set, we observed that the BRD4 interactions with CDK9 and CCNT1 reduced significantly for BRD4 P536A mutant or on PHD2 knockdown (Fig. 3*B*–3*D*, Supplemental Fig. S5*B*). More importantly, the difference in BRD4 interactions with CDK9 and CCNT1 between BRD4 WT and P536A mutant was obliterated on PHD2 knockdown (supplemental Fig. S5*C*). And unlike the BRD4 WT, the interaction of BRD4 P536A mutant with the P-TEFb complex was unaffected by PHD2 knockdown (supplemental Fig. S5*D*). Such consistent observations from the analysis of both enzyme-mediated inhibition of BRD4 proline hydroxylation and site-specific mutations suggested that PHD2-BRD4 regulatory axis promotes BRD4 interactions with key transcription factors and therefore, likely affect BRD4-dependant gene transcription.

To validate these findings, we performed coimmunoprecipitation and Western blot analysis. Comparing to the wild-type BRD4, both site-specific inhibition of proline hydroxylation with BRD4 mutant and chemical inhibition of prolyl hydroxylase activity with DMOG significantly decreased the interaction of BRD4 with CDK9, CDK1, and MCM5, respectively (Fig. 4*A*). We further confirmed that specific inhibition of PHD2 via shRNA knockdown also led to a significant decrease of the BRD4 interaction with specific binding protein CDK9. Overall, these data confirmed the findings from the quantitative inter-

actome analysis and demonstrated that site-specific proline hydroxylation regulates BRD4 interactions with key transcription factors.

Proline Hydroxylation-mediated BRD4 Transcriptional Activity—To determine the role of site-specific proline hydroxylation in BRD4 transcriptional activity, we developed a luciferase reporter assay. The assay involved the expression of a luciferase plasmid with a promoter of the endogenous c-myc gene and quantification with a Dual-Luciferase reporter system. As positive controls, we showed that the treatment of 293T cells with JQ1 (a known bromodomain inhibitor) (46) or specific inhibition of BRD4 with siRNA led to significantly reduced c-myc promoter activity and luciferase expression through luciferase assays. Then we performed a rescue experiment by overexpression of WT or mutant BRD4 P536A with a concomitant knockdown of endogenous BRD4. Our results showed that expression of BRD4 mutant failed to enhance the luciferase assay activity to the same extent compared with the BRD4 wild-type, suggesting that site-specific inhibition of BRD4 P536 hydroxylation strongly affected BRD4 transcriptional activity (Fig. 4*C*). To further validate the role of site-specific proline hydroxylation in BRD4 transcriptional activity *in vivo*, we applied quantitative PCR assay. We first screened several known BRD4 targets through BRD4 shRNA knockdown and qPCR assay. We found CCND1, a cell cycle regulatory protein, was the most representative BRD4 target in 293T cells and Hela cells. Then we performed a rescue experiment by overexpression of wild-type or mutant BRD4 P536A in the 293T cells with the concomitant knockdown of endogenous BRD4. Our results showed that the expression of WT BRD4 partially rescued the expression of CCND1 but not BRD4 P536A mutant (Fig. 4*D*). Accordingly, knockdown of PHD2, the regulatory enzyme of BRD4 proline hydroxylation led to a significant reduction in CCND1 gene expression (Fig. 4*E*). These data confirmed that inhibition of BRD4 proline hydroxylation strongly affected BRD4-dependent transcriptional activity *in vivo*.

DISCUSSION

In the present study, we applied PRM-based targeted quantitation and *in vivo* enzymatic assays to identify PHD2 as the major regulatory enzyme of BRD4 proline hydroxylation. In contrast to the well-known Hyp targets such as HIF-α, we found that proline hydroxylation on BRD4 does not affect its degradation or protein abundance. Using label-free quantitative interactome analysis, we determined that PHD2-dependent site-specific proline hydroxylation on BRD4 mediates protein-protein interactions of BRD4 with key transcription factors and inhibition of site-specific BRD4 proline hydroxylation reduced BRD4-mediated transcriptional activation. Taken together, our findings established PHD2-BRD4 regulatory axis as a functionally significant pathway for BRD4-dependent gene activation and cell proliferation.

Proline hydroxylation is an essential posttranslational modification that mediates the metabolic sensing pathways in eukaryotic cells. Hydroxylation of proline at C-4 affects the cis-trans isomerization of proline peptide bonds because of the *gauche* effect and therefore regulates the secondary structure of the substrate proteins (10). Our studies revealed that BRD4 proline hydroxylation regulates BRD4 interactions with specific binding proteins, and potentially affects BRD4-mediated gene transcription. Interestingly, the hydroxylation site on BRD4 is located at a junction between the phosphorylation-rich NPS domain and lysine-rich BID domain (47). Although the exact mechanism remains to be determined, it is reasonable to speculate that BRD4 Hyp modification may regulate the folding or the interdomain interactions of BRD4, which may affect downstream protein-protein interactions and signaling.

Chemical inhibition of prolyl hydroxylases is a promising strategy to regulate proline hydroxylation pathways in cells and tissues. Our previous analysis found that specific chemical inhibition of PHD-mediated proline hydroxylation pathway significantly inhibited the expression of BRD4-target c-Myc and cell proliferation in Acute Myeloid Leukemia (AML). Accordingly, gene expression analysis of TCGA database (http://cancergenome.nih.gov/) showed that PHD2 but not PHD1 or PHD3 is significantly overexpressed in AML patient (supplemental Fig. S7). Patient with rapid progression of AML also shows significantly higher levels of PHD2 expression (supplemental Fig. S7). This evidence suggest that PHD2-mediated proline hydroxylation is a potential oncogenic pathway in AML that drives BRD4-mediated gene expression, as well as cancer cell proliferation and specific inhibition of PHD2 activity with chemical inhibitors, may serve as a new alternative strategy in AML treatment. Indeed, recent clinical applications of prolyl hydroxylase inhibitors for the treatment of ischemic diseases (48–50) and anemia (51) suggest that prolyl hydroxylase inhibitors are generally safe in humans. Therefore, our identification of PHD2-BRD4 regulatory axis may provide new insights to develop more potent and effective chemical interventions for therapeutic applications and treatment of diseases such as AML.

Acknowledgments—We thank Do-Hyung Kim, Peter Gordon, Timothy Griffin and the members of the Chen lab for helpful suggestions and discussion. We are grateful to the University of Minnesota's Center for Mass Spectrometry and Proteomics for LC-MS instrument access and support.

DATA AVAILABILITY

The mass spectrometry proteomics data have been deposited to the ProteomeXchange Consortium via the PRIDE partner repository (52) with the data set identifier PXD012633 and PXD012674.

* This work was supported by the University of Minnesota research start-up fund (to Y.C.) and the National Institute of Health (1R35GM124896 to Y.C.).

S This article contains supplemental material.

‡To whom correspondence should be addressed. E-mail: YueChen@umn.edu.

Author contributions: L.N.E. and A.L. performed research; L.N.E. and A.L. analyzed data; L.N.E. and Y.C. wrote the paper; Y.C. designed research.

REFERENCES

1. Ivan, M., and Kaelin, W. G. (2017) The EGLN-HIF O_2-sensing system: multiple inputs and feedbacks. *Mol. Cell.* **66,** 772–779
2. Semenza, G. L. (2014) Oxygen sensing hypoxia-inducible factors and disease pathophysiology. *Annu. Rev. Pathol. Mech. Dis.* **9,** 47–71
3. Schofield, C. J., and Ratcliffe, P. J. (2004) Oxygen sensing by HIF hydroxylases. *Nat. Rev. Mol. Cell Biol.* **5,** 343–354
4. Wong, B. W., Kuchnio, A., Bruning, U., and Carmeliet, P. (2013). Emerging novel functions of the oxygen-sensing prolyl hydroxylase domain enzymes. *Trends Biochem. Sci.* **38,** 3–11
5. Zhang, J., and Zhang, Q. (2018) VHL and hypoxia signaling: beyond HIF in Cancer. *Biomedicines* **6,** 35
6. Ivan, M., Kondo, K., Yang, H., Kim, W., Valiando, J., Ohh, M., Salic, A., Asara, J. M., Lane, W. S., and Kaelin, W. G. (2001) HIFalpha targeted for VHL-mediated destruction by proline hydroxylation: implications for O2 sensing. *Science* **292,** 464–468
7. Jaakkola, P., Mole, D. R., Tian, Y.-M., Wilson, M. I., Gielbert, J., Gaskell, S. J., Av. Kriegsheim Hebestreit, H. F., Mukherji, M., Schofield, C. J., Maxwell, P. H., Pugh, C. W., and Ratcliffe, P. J. (2001) Targeting of HIF-alpha to the von Hippel-Lindau ubiquitylation complex by O2-regulated prolyl hydroxylation. *Science* **292,** 468–472
8. Yu, F., White, S. B., Zhao, Q., and Lee, F. S. (2001) HIF-1alpha binding to VHL is regulated by stimulus-sensitive proline hydroxylation. *Proc. Natl. Acad. Sci. USA* **98,** 9630–9635
9. Masson, N., Willam, C., Maxwell, P. H., Pugh, C. W., and Ratcliffe, P. J. (2001) Independent function of two destruction domains in hypoxia-inducible factor-alpha chains activated by prolyl hydroxylation. *EMBO J.* **20,** 5197–5206
10. Gorres, K. L., and Raines, R. T. (2010) Prolyl 4-hydroxylase. *Crit. Rev. Biochem. Mol. Biol.* **45,** 106–124
11. Ratcliffe, P. J. (2013) Oxygen sensing and hypoxia signalling pathways in animals: the implications of physiology for cancer. *Physiol. J.* **591,** 2027–2042
12. Schonenberger, M. J., and Kovacs, W. J. (2015) Hypoxia signaling pathways: modulators of oxygen-related organelles. *Front. Cell Dev. Biol.* **3,** 42
13. Haase, V. H. (2013) Regulation of erythropoiesis by hypoxia-inducible factors. *Blood Rev.* **27,** 41–53
14. Krock, B. L., Skuli, N., and Simon, M. C. (2011) Hypoxia-induced angiogenesis: good and evil. *Genes Cancer* **2,** 1117–1133
15. Epstein, A. C. R., Gleadle, J. M., McNeill, L. A., Hewitson, K. S., O'Rourke, J., Mole, D. R., Mukherji, M., Metzen, E., Wilson, M. I., Dhanda, A., Tian, Y.-M., Masson, N., Hamilton, D. L., Jaakkola, P., Barstead, R., Hodgkin, J., Maxwell, P. H., Pugh, C. W., Schofield, C. J., and Ratcliffe, P. J. (2001) Celegans EGL-9 and mammalian homologs define a family of dioxygenases that regulate HIF by prolyl hydroxylation. *Cell* **107,** 43–54
16. Bruick, R. K. (2001) A conserved family of prolyl-4-hydroxylases that modify, H. I. F. *Science* **294,** 1337–1340
17. Berra, E., Benizri, E., Ginouves, A., Volmat, V., Roux, D., and Pouyssegur, J. (2003) HIF prolyl-hydroxylase 2 is the key oxygen sensor setting low steady-state levels of HIF-1 alpha in normoxia. *EMBO J.* **22,** 4082–4090
18. Lieb, M. E., Menzies, K., Moschella, M. C., Ni, R., and Taubman, M. B. (2002) Mammalian EGLN genes have distinct patterns of mRNA expression and regulation. *Biochem. Cell Biol.* **80,** 421–426
19. Maxwell, P. H., Wiesener, M. S., Chang, G.-W., Clifford, S. C., Vaux, E. C., Cockman, M. E., Wykoff, C. C., Pugh, C. W., Maher, E. R., and Ratcliffe, P. J. (1999) The tumour suppressor protein VHL targets hypoxia-inducible factors for oxygen-dependent proteolysis. *Nature* **399,** 271–275
20. Ohh, M., Park, C. W., Ivan, N., Hoffman, M. A., Kim, T. Y., Huang, L. E., Pavletich, N., Chau, V., and Kaelin, W. G. (2000) Ubiquitination of hypoxia-inducible factor requires direct binding to the beta-domain of the von Hippel-Lindau protein. *Nat. Cell Biol.* **2,** 423–427
21. Hon, W. C., Wilson, M. I., Harlos, K., Claridge, T. D. W., Schofield, C. J., Pugh, C. W., Maxwell, P. H., Ratcliffe, P. J., Stuart, D. I., and Jones, E. Y. (2002) Structural basis for the recognition of hydroxyproline in alpha IF-1 alpha by pVHL. *Nature* **417,** 975–978
22. Min, J. H., Yang, H. F., Ivan, M., Gertler, F., Kaelin, W. G., and Pavletich, N. P. (2002) Structure of an HIF-1 alpha-pVHL complex: Hydroxyproline recognition in signaling. *Science* **296,** 1886–1889
23. Semenza, G. L. (2001) Hypoxia-inducible factor 1: oxygen homeostasis and disease pathophysiology. *Trends Mol. Med.* **7,** 345–350
24. Semenza, G. L., and Wang, G. L. (1992) A nuclear factor induced by hypoxia via denovo protein-synthesis binds to the human erythropoietin gene enhancer at a site required for transcriptional activation. *Mol. Cell Biol.* **12,** 5447–5454
25. Wang, G. L., Jiang, B. H., Rue, E. A., and Semenza, G. L. (1995) Hypoxia-inducible factor 1 is a basic-helix-loop-helix-PAS heterodimer regulated by cellular O2 tension. *Proc. Natl. Acad Sci.* **92,** 5510–5514
26. Luo, W., Hu, H., Chang, R., Zhong, J., Knabel, M., O'Meally, R., Cole, R., Pandey, A., and Semenza, G. (2011) Pyruvate kinase M2 is a PHD3-stimulated coactivator for hypoxia-inducible factor 1. *Cell.* **145,** 732–744
27. Zheng, X., Zhai, B., Koivunen, P., Shin, S. J., Lu, G., Liu, J., Geisen, C., Chakraborty, A. A., Moslehi, J. J., Smalley, D. M., Wei, X., Chen, X., Chen, Z., Beres, J. M., Zhang, J., Tsao, J. L., Brenner, M. C., Zhang, Y., Fan, C., DePinho, R. A., Paik, J., Gygi, S. P., Kaelin, W. G., and Zhang, Q. (2014) Prolyl hydroxylation by EglN2 destabilizes FOXO3a by blocking its interaction with the USP9x deubiquitinase. *Genes Dev.* **28,** 1429–1444
28. Lee, D. C., Sohn, H. A., Park, Z. Y., Oh, S., Kang, Y. K., Lee, K. M., Kang, M., Jang, Y. J., Yang, S. J., Hong, Y. K., Noh, H., Kim, J. A., Kim, D. J., Bae, K. H., Kim, D. M., Chung, S. J., Yoo, H. S., Yu, D. Y., Park, K. C., Il and Yeom, Y. (2015) A lactate-induced response to hypoxia. *Cell.* **161,** 595–609
29. Guo, J., Chakraborty, A. A., Liu, P., Gan, W., Zheng, X., Inuzuka, H., Wang, B., Zhang, J., Zhang, L., Yuan, M., Novak, J., Cheng, J. Q., Toker, A., Signoretti, S., Zhang, Q., Asara, J. M., Kaelin, W. G., and Wei, W. (2016) pVHL suppresses kinase activity of Akt in a proline-hydroxylation-dependent manner. *Science* **353,** 929–932
30. German, N. J., Yoon, H., Yusuf, R. Z., Murphy, J. P., Finley, L. W. S., Laurent, G., Haas, W., Satterstrom, F. K., Guarnerio, J., Zaganjor, E., Santos, D., Pandolfi, P. P., Beck, A. H., Gygi, S. P., Scadden, D. T., Kaelin, W. G., and Haigis, M. C. (2016) PHD3 loss in cancer enables metabolic reliance on fatty acid oxidation via deactivation of ACC2. *Mol. Cell.* **63,** 1006–1020
31. Rodriguez, J., Herrero, A., Li, S., Rauch, N., Quintanilla, A., Wynne, K., Krstic, A., Acosta, J. C., Taylor, C., Schlisio, S., and von Kriegsheim, A. (2018) PHD3 Regulates p53 protein stability by hydroxylating proline 359. *Cell Rep.* **24,** 1316–1329
32. Zhou, T., Erber, L., Liu, B., Gao, Y., Ruan, H.-B., and Chen, Y. (2016) Proteomic analysis reveals diverse proline hydroxylation-mediated oxygen-sensing cellular pathways in cancer cells. *Oncotarget.* **7,** 79154–79169
33. Moser, S. C., Bensaddek, D., Ortmann, B., Maure, J., Mudie, S., Blow, J. J., Lamond, A. I., Swedlow, J. R., and Rocha, S. (2013) Article PHD1 links cell-cycle progression to oxygen sensing through hydroxylation of the centrosomal protein Cep192. *Dev. Cell.* **26,** 381–392
34. Shevchenko, A., Tomas, H., Havli, J., Olsen, J. V., and Mann, M. (2007) In-gel digestion for mass spectrometric characterization of proteins and proteomes. *Nat. Protoc.* **1,** 2856
35. Cox, J., and Mann, M. (2008) MaxQuant enables high peptide identification rates, individualized p. p. b.-range mass accuracies and proteome-wide protein quantification. *Nat. Biotechnol.* **26,** 1367
36. Tyanova, S., Temu, T., Sinitcyn, P., Carlson, A., Hein, M. Y., Geiger, T., Mann, M., and Cox, J. (2016) The Perseus computational platform for comprehensive analysis of (prote)omics data. *Nat. Methods* **13,** 731–740
37. Cox, J., Hein, M. Y., Luber, C. A., Paron, I., Nagaraj, N., and Mann, M. (2014) Accurate proteome-wide label-free quantification by delayed normalization and maximal peptide ratio extraction termed MaxLFQ. *Mol. Cell. Proteomics* **13,** 2513–2526
38. Christin, C., Hoefsloot, H. C. J., Smilde, A. K., Hoekman, B., Suits, F., Bischoff, R., and Horvatovich, P. (2013) A critical assessment of feature selection methods for biomarker discovery in clinical proteomics. *Mol. Cell. Proteomics* **12,** 263–276
39. Peterson, A. C., Russell, J. D., Bailey, D. J., Westphall, M. S., and Coon, J. J. (2012) Parallel reaction monitoring for high resolution and high mass

accuracy quantitative targeted proteomics. *Mol. Cell. Proteomics* **11,** 1475–1488

40. Huang, D. W., Sherman, B. T., and Lempicki, R. A. (2009) Systematic and integrative analysis of large gene lists using DAVID bioinformatics resources. *Nat. Protoc.* **4,** 44–57
41. Huang, D. W., Sherman, B. T., and Lempicki, R. A. (2009) Bioinformatics enrichment tools: paths toward the comprehensive functional analysis of large gene lists. *Nucleic Acids Res.* **37,** 1–13
42. Shannon, P. (2003) Cytoscape: ASoftware environment for integrated models of biomolecular interaction networks. *Genome Res.* **13,** 2498–2504
43. Rodriguez, J., Pilkington, R., Garcia Munoz, A., Nguyen, L., Rauch, N., Kennedy, S., Monsefi, N., Herrero, A., Taylor, C., and von Kriegsheim, A. (2016) Substrate-trapped interactors of PHD3 and FIHCluster in distinct signaling pathways. *Cell Rep.* **14,** 2745–2760
44. Fujisawa, T., and Filippakopoulos, P. (2017) Functions of bromodomain-containing proteins and their roles in homeostasis and cancer. *Nat. Rev. Mol. Cell Biol.* **18,** 246–262
45. Mertz, J. A., Conery, A. R., Bryant, B. M., Sandy, P., Balasubramanian, S., Mele, D. A., Bergeron, L., and Sims, R. J. (2011) Targeting MYC dependence in cancer by inhibiting BET bromodomains. *Proc. Natl. Acad. Sci.* **108,** 16669–16674
46. Filippakopoulos, P., Qi, J., Picaud, S., Shen, Y., Smith, W. B., Fedorov, O., Morse, E. M., Keates, T., Hickman, T. T., Felletar, I., Philpott, M., Munro, S., McKeown, M. R., Wang, Y., Christie, A. L., West, N., Cameron, M. J., Schwartz, B., Heightman, T. D., La Thangue, N., French, C. A., Wiest, O., Kung, A. L., Knapp, S., and Bradner, J. E. (2010) Selective inhibition of BET bromodomains. *Nature* **468,** 1067–1073
47. Wu, W., Lee, A., Lai, H., Zhang, H., and Chiang, C. (2013) Phospho switch triggers Brd4 chromatin binding and activator recruitment for gene-specific targeting. *Mol. Cell* **49,** 843–857
48. Schneider, M., Harnoss, J. M., Strowitzki, M. J., Radhakrishnan, P., Platzer, L., Harnoss, J. C., Hank, T., Cai, J., and Ulrich, A. (2015) Therapeutic inhibition of prolyl hydroxylase domain-containing enzymes in surgery: putative applications and challenges. *Hypoxia* **3,** 1–14
49. Sen Banerjee, S., Thirunavukkarasu, M., Rishi, M. T., Sanchez, J. A., Maulik, N., and Maulik, G. (2012) HIF prolyl hydroxylases and cardiovascular diseases. *Toxicol. Mech. Methods* **22,** 347–358
50. Zhou, J., Li, J., Rosenbaum, D. M., Zhuang, J., Poon, C., Qin, P., Rivera, K., Lepore, J., Willette, R. N., Hu, E., and Barone, F. C. (2017) The prolyl 4-hydroxylase inhibitor GSK360A decreases post-stroke brain injury and sensory, motor, and cognitive behavioral deficits. *PLoS ONE* **12,** e0184049
51. Joharapurkar, A. A., Pandya, V. B., Patel, V. J., Desai, R. C., and Jain, M. R. (2018) Prolyl hydroxylase inhibitors: a breakthrough in the therapy of anemia associated with chronic diseases. *Med. J. Chem.* **61,** 6964–6982
52. Perez-Riverol, Y., Csordas, A., Bai, J., Bernal-Llinares, M., Hewapathirana, S., Kundu, D. J., Inuganti, A., Griss, J., Mayer, G., Eisenacher, M., Pérez, E., Uszkoreit, J., Pfeuffer, J., Sachsenberg, T., Ş. Yılmaz Tiwary, S., Cox, J., Audain, E., Walzer, M., Jarnuczak, A. F., Ternent, T., Brazma, A., and Vizcaíno, J. A. (2018) The PRIDE database and related tools and resources in 2019: improving support for quantification data. *Nucleic Acids Res.* **47,** 442–450